The impact of thickness heterogeneity on soft tissue biomechanics: A novel measurement technique and a demonstration on heart valve tissue

Chien-Yu Lin
The University of Texas at Austin
Mrudang Mathur
The University of Texas at Austin
Marcin Malinowski
Spectrum Health
Tomasz A. Timek
Spectrum Health
Manuel K. Rausch (manuel.rausch@utexas.edu)
The University of Texas at Austin

Research Article

Keywords: Mitral Valve, Optical Profilometry, Mechanical Testing, Biaxial Tension, Bending, Buckling

Posted Date: June 16th, 2022

DOI: https://doi.org/10.21203/rs.3.rs-1751351/v1

The impact of thickness heterogeneity on soft tissue biomechanics: A novel measurement technique and a demonstration on heart valve tissue

Chien-Yu Lin[1] · Mrudang Mathur[2] · Marcin Malinowski[3,4] · Tomasz A. Timek[3] · Manuel K. Rausch[1,5,6]

Received: date / Accepted: date

Abstract The mechanical properties of soft tissues are driven by their complex, heterogeneous composition and structure. Interestingly, studies of soft tissue biomechanics often ignore spatial heterogeneity. In our work, we are therefore interested in exploring the impact of tissue heterogeneity on the mechanical properties of soft tissues. Therein, we specifically focus on soft tissue heterogeneity arising from spatially-varying thickness. To this end, our first goal is to develop a non-destructive measurement technique that has a high spatial resolution, provides continuous thickness maps, and is fast. Our secondary goal is to demonstrate that including spatial variation in thickness is important to the accuracy of biomechanical analyses. To this end, we use mitral valve leaflet tissue as our model system. To attain our first goal, we identify a soft tissue-specific contrast protocol that enables thickness measurements using a Keyence profilometer. We also show that this protocol does not affect our tissues' mechanical properties. To attain our second goal, we conduct virtual biaxial, bending, and buckling tests on our model tissue both ignoring and considering spatial variation in thickness. Thereby, we show that the assumption of average, homogeneous thickness distributions significantly alters the results of biomechanical analyses when compared to including true, spatially-varying thickness distributions. In conclusion, our work provides a novel measurement technique that can capture continuous thickness maps non-invasively, at high resolution, and in short time. Our work also demonstrates the importance of including heterogeneous thickness in biomechanical analyses of soft tissues.

Keywords Mitral Valve · Optical Profilometry · Mechanical Testing · Biaxial Tension · Bending · Buckling

Manuel K. Rausch
E-mail: manuel.rausch@utexas.edu

1 Department of Biomedical Engineering, University of Texas at Austin, Austin, TX 78712, USA

2 Department of Mechanical Engineering, University of Texas at Austin, TX 78712, USA

3 Division of Cardiothoracic Surgery, Spectrum Health, Grand Rapids, MI 49503, USA

4 Department of Cardiac Surgery, School of Medicine in Katowice, Medical University of Silesia, Katowice, Poland

5 Department of Aerospace Engineering and Engineering Mechanics, University of Texas at Austin, Austin, TX 78712, USA

6 Oden Institute for Computational Engineering and Sciences, University of Texas at Austin, Austin, TX 78712, USA

1 Introduction

Characterizing and predicting the mechanical properties of soft tissues is critical to our understanding of health and disease [8,34,18]. These properties are often driven by soft tissues' complex, heterogeneous composition and structure [3,7,9]. That is, soft tissues are usually organized in layers with each layer showing distinct and spatially-varying properties. Of course, this is common knowledge [21,4,33]. It is therefore noteworthy that, with few exceptions, many studies ignore heterogeneity when conducting mechanical analyses of soft tissues, including some of our own [31,28,19]. The reason likely being that measuring spatially-varying properties is hard and time consuming, with benefits often

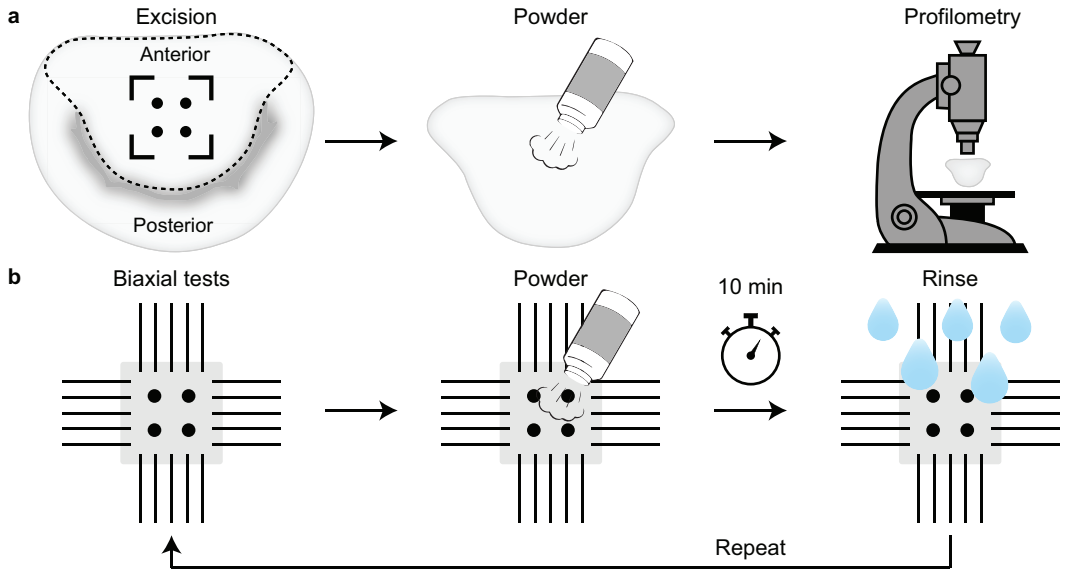

Fig. 1 Experimental overview. a) We excised the anterior leaflet of n=6 ovine mitral valves and applied talcum powder for optical contrast. Next, we imaged each sample using a Keyence profilometer to create high-resolution, spatial thickness maps of our samples. b) Next, we tested whether the application of talcum powder and a 10-minute imaging period negatively affects the tissues' mechanics. To this end, we measured the biaxial properties of the anterior leaflets before and after applying powder for 10 minutes.

unknown. In our current work, we are therefore interested in exploring and highlighting the impact of tissue heterogeneity on biomechanical analyses of soft tissues. Therein, we specifically focus on soft tissue heterogeneity arising from spatially-varying thickness.

Our interest in exploring heterogeneity in tissue thickness was first sparked during a recent computational study of the human tricuspid valve in which we assumed that each leaflet had a uniform thickness [20]. We made this assumptions because creating an accurate, spatially-varying thickness map appeared non-feasible with our available thickness measurement techniques. In the course of said modeling work, we found that the simulated heart valves folded in rather unnatural locations. Thus, we re-inspected the original tissue and found that native heart valve leaflets tended to be significantly thinner in those regions that undergo folding, while being thicker in those regions that aren't meant to fold. In other words, native tissue had a non-uniform thickness distribution. From an engineering perspective, this is an entirely logical design with thinner areas being a nucleus for folding and buckling [16,17]. To overcome the limitation of our work, we began a quest for a technique to measure spatially-varying tissue thickness and to provide strong support for the inclusion of heterogeneity in thickness – and other physical properties – in biomechanical analyses.

Of course, there are many means to measure tissue thickness [24,10]. However, none we found fulfilled our need for i) being non-destructive, ii) having a high spatial resolution, iii) providing continuous spatial maps, and iv) being fast. For example, histology-based methods are destructive and provide thickness measurements only within two-dimensional layers [32,30], gauges and calipers only provide focal measurements [5,14], while ultrasound has a limited spatial resolution and optical coherence tomography is limited in depth [23,1,2]. The first goal of our work is therefore to introduce a technique that fulfills needs i)-iv) and to demonstrate this technique on heart valve tissue. Our second goal is to demonstrate the importance of including tissue heterogeneity in biomechanical analyses via virtual planar biaxial tests, bending tests, and a buckling mode analysis; again, by example of heart valve tissue.

2 Methods

2.1 Tissue origin and preparation

We isolated anterior mitral valve leaflets from n=6 healthy male Dorset sheep, 51 ± 8 kg aged 5–6 months, and cryogenically stored the tissue at -80^{o}C in a 9:1 ratio of DMEM:DMSO with protease inhibitor until final testing [22]. Immediately before testing, we rapidly thawed the leaflets to room temperature and photographed them while they floated on a layer of 1× PBS. We used a background grid for calibration.

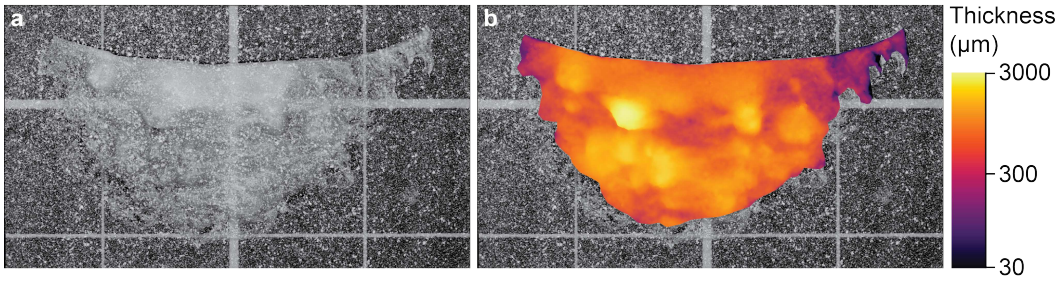

Fig. 2 High-resolution thickness map of an anterior mitral valve leaflet via optical profilometry. a) Raw image of an anterior mitral valve leaflet with talcum powder. b) Raw image with profilometry-based thickness map superimposed. Please note, thickness data is mapped to a logarithmic scale.

2.2 Tissue profilometry

After taking photos of a thawed anterior mitral valve leaflet, we gently dried it using absorbent tissue (KimWipes, Kimberly-Clark, Irving, TX, USA). Next, we covered the tissue with microfine talc granules suspended with a trace of lanolin (PowderPen, NextEngine, CA, USA) to minimize tissue glare and to reduce the tissue's optical transparency. Finally, we created a 3D thickness map of the leaflet using an optical profilometer (VHX-5000, Keyence, Osaka, Japan) under 50× magnification. To validate the accuracy of our tissue profilometry, we also measured the thickness of a rubber sample in multiple regions with a digital thickness gauge (547-500S, Mitutoyo Corp., Kawasaki, Japan) and subsequently imaged the same sample with the Keyence scope to obtain its spatial thickness map for comparison.

2.3 Biaxial testing

To ensure that our profilometry protocol did not have spurious effects on tissue mechanics, we performed repeated biaxial testing on a separate set of tissues: once before and once after powder application, **Figure 1**. Specifically, we isolated a 7 mm × 7 mm square from the belly regions of n = 6 anterior mitral valve leaflets. Before mounting the tissues to our planar biaxial tester, we marked the atrialis surface of each sample with ink dots in a 3 mm × 3 mm square pattern. Floating on 1× PBS, we took images of this pattern for later use. Next, we mounted the samples on our biaxial device (Biotester, Cellscale, Waterloo, ON, Canada) and tested the samples twice without dismounting them: First, in 37 °C 1× PBS, after which we gently dried the sample with absorbent tissue (KimWipes) and applied the same powder to the sample as used in preparation for imaging. Subsequently, we let the sample air-dry for 10 minutes (the length of our imaging protocol), before carefully cleaning the sample with 1× PBS and performing a second set of mechanical tests in 37 °C 1× PBS. Between tests we did not zero the load cells (1.5 N capacity, ± 1.5 mN) and tests began from identical motor positions. During both tests, we performed 10 preconditioning cycles equibiaxially to 500 mN, preloaded the tissue to 10 mN to remove any slack, and then conducted two final equibiaxial cycles to 500 mN. While testing, we recorded the rake-to-rake distances, radial and circumferential forces, and fiduciary marker images at 5 Hz. Using the fiduciary marker positions on the tissue throughout testing, we calculated the deformation gradient tensor, $\mathbf{F}$, with respect to the floating stress-free reference configuration. In turn, we acquired in-plane stretches from the right Cauchy-Green deformation tensor, $\mathbf{C} = \mathbf{F}^T\mathbf{F}$, and calculated the membrane tension as the force divided by the rake-to-rake distance in the deformed configuration. To characterize the resulting nonlinear tension-stretch curves, we also computed four scalar metrics: Toe Stiffness (i.e., lower region slope), Calf Stiffness (i.e., upper region slope), Transition Stretch (i.e., stretch data point nearest to intersection of lower and upper region slope), and Degree of Anisotropy (i.e., the ratio between the circumferential and radial stretches at $50\,\mathrm{N\,m^{-1}}$) [25,15,26, 21].

2.4 Numerical experimentation

To determine the effects of heterogeneity in thickness on the biomechanics of soft tissues, we numerically analysed mitral valve tissue samples under biaxial tension, bending, and buckling. To this end, we first identified three square areas of size 7 mm × 7 mm in the spatial thickness maps of our anterior mitral valve leaflet. We then discretized these squares with shell elements and used a custom MATLAB code (MATLAB v2021b, Mathworks, Natick, MA) to map the heterogeneous thicknesses onto the shells. For the constitutive model, we chose a Neo-Hookean material with shear modulus $\mu = 20\,\mathrm{MPa}$ [27]. Subsequently, we imported the

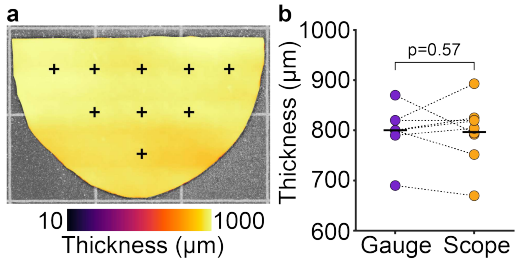

Fig. 3 Validation of our optical profilometry technique against digital thickness gauge measurements of a rubber sample. Please note, '+' demarks the gauge measurements points and thickness data is mapped to a logarithmic scale.

discretized geometries into ABAQUS/Standard (Dassault Systemes, Providence, RI) and analyzed them under biaxial stretch, bending, and buckling using the finite element method. To biaxially test the samples, we simultaneously applied a stretch of 1.5 to all four edges of the domains. For the bending analysis, we clamped one edge of our domains and applied a moment $M = 4 \times 10^{-2}\,\mathrm{N\,m}$ to the opposite edge [13]. To model the buckling response of the samples, we used a linear perturbation analysis in ABAQUS. Here, we clamped the edges of our sample and applied a pressure load of $P = 0.2\,\mathrm{MPa}$ to the bottom surface of our domains as boundary conditions [6]. Finally, we repeated these simulations but assumed that the samples had a homogeneous, average thickness distributions rather than the true, spatially-varying thickness distributions.

2.5 Statistics

To test whether our profilometry protocol affected the biomechanics of our test samples, we compared four mechanical metrics before and after applying the protocol. Because the mechanical tests were performed on the same samples, we used a two-sided, dependent Student t-test. We conducted these statistical analyses in MATLAB where we assumed that a p-value smaller than 0.05 would be significant. Where applicable, we report values as mean ± 1 standard deviation.

3 Results

3.1 Optical profilometry yields continuous, high-resolution thickness map of an anterior mitral valve leaflet

We successfully applied the powder strategy to our test sample and obtained a continuous, high-resolution thickness map of an anterior mitral valve leaflet, see **Figure 2**. That is, our contrast technique successfully enabled the autofocus-based thickness mapping of the profilometer. Additionally, we found that profilometry-derived thickness values matched the gold-standard technique (i.e., a thickness gauge) very well, see **Figure 3**. Specifically, the difference between the two methods was $10 \pm 27\,\mu\mathrm{m}$, equivalent to a mean error of 1.26%.

3.2 Our profilometry protocol does not change the mechanical properties of anterior mitral valve leaflets

To evaluate the effects of our profilometry protocol on tissue mechanics, we equibiaxially tested n = 6 square samples from mitral valve anterior leaflets in a dependent experimental design (i.e., repeat testing of the same samples before and after using the profilometry protocol). We found that all samples, before and after applying the profilometry protocol, exhibited classic non-linear J-shaped loading behavior, as expected for collagenous tissues, see **Figure 4a**. Qualitatively, the stress-stretch curves in radial and circumferential direction looked identical between both groups. Additionally we quantified the Toe Stiffness, Calf Stiffness, Transition Stretch, and Degree of Anisotropy. When comparing those values, we found no statistically significant differences in any of the metrics, see **Figure 4c**. Overall, our profilometry protocol appeared to not affect our tissues' mechanics.

3.3 Assuming homogeneity accrues significant errors in the biaxial response of an anterior mitral valve leaflet

To determine the effects of spatially-varying thickness on soft tissue biomechanics, we simulated the deformation of three anterior mitral valve leaflet samples under biaxial tension. Each samples was virtually excised from our continuous thickness map as shown in **Figure 2**. In our analysis, we compared results under the assumption of thickness homogeneity to results obtained with the true, spatially-varying thickness distributions, see **Figure 5**. First, we found that reaction forces varied based on where the samples were excised. In other words, thickness heterogeneity induced intra-subject variability. Additionally, for a given sample we found that the assumption of homogeneity overestimated material stiffness when compared to the samples with heterogeneous thicknesses. Moreover, thickness heterogeneity induced anisotropy in the mechanical response of our tissues, even when using an isotropic material model. Together, errors in the predicted tension-stretch behavior of our samples due to the assumption of homogeneity were as large as 21% depending on sample location and material direction. Of course, we also found

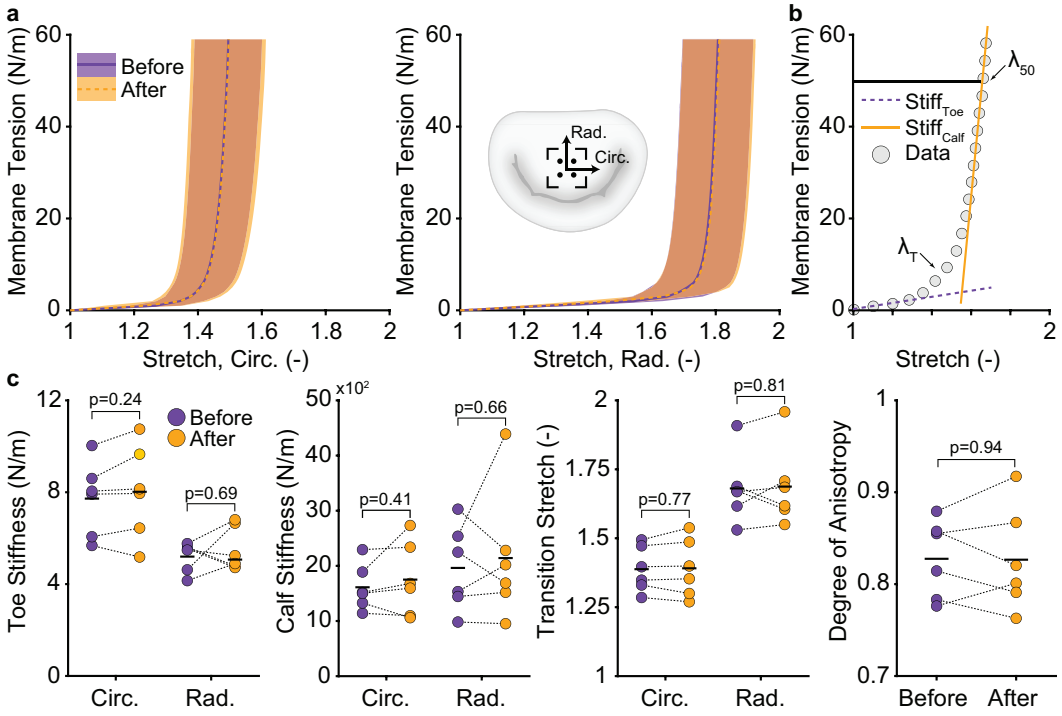

Fig. 4 Our profilometry protocol does not affect the biaxial mechanics of anterior mitral valve leaflets. a) Tension-stretch curves in circumferential and radial direction before and after applying talcum powder and dehydrating for 10 minutes. b) Explanation of four quantitative metrics of the biaxial tissue mechanics: Toe Stiffness ($\text{Stiff}_{\text{Toe}}$), Calf Stiffness ($\text{Stiff}_{\text{Calf}}$), Transition Stretch ($\lambda_{\text{T}}$), and Degree of Anisotropy (λ_{50} in circumferential direction divided by λ_{50} in radial direction.) c) Quantitative comparison of the biaxial mechanics of anterior mitral valve leaflets before and after applying our profilometry protocol.

that predicted stresses varied spatially when considering thickness heterogeneity, while the assumption of homogeneity lead to homogeneous stress fields, see **Figure 6a**. Quantitatively, we found stress distributions across all finite elements in our heterogeneous samples of 50 ± 20 MPa in Sample 1, 52 ± 19 MPa in Sample 2, and 50 ± 21 MPa in Sample 3. In contrast, each sample with homogeneous thickness had a uniform stress value of 41 MPa. In other words, errors in mean stress were as large as 26% when ignoring heterogeneity in tissue thickness.

3.4 Assuming homogeneity also accrues significant errors in the bending response of an anterior mitral valve leaflet

To determine the effects of spatially-varying thickness on soft tissue biomechanics, we also simulated the deformation of three virtual anterior mitral valve leaflet samples under bending. To this end, we used the same virtual samples as above and simulated their mechanical response assuming homogeneity or applying true, spatially-varying thickness distributions. As with the biaxial tension tests, we found that the bending response varied between samples, i.e., spatially-varying thickness also introduced intra-subject variability in bending stiffness. Again, as we with the biaxial tension test, we found that the assumption of homogeneity overestimates the material stiffness when compared to the sample with heterogeneous thicknesses, see **Table 1**. The resulting errors in predicted free-edge displacement were as large as 61% and 19% in the X- and Y-directions, respectively. Because bending is a heterogeneous deformation, we found spatially-varying element stresses in both cases: when assuming homogeneity and when applying true, spatially-varying thickness distributions, see **Figure 6b**. However, we found significantly more spatial variability in the latter case than in the former case. Quantitatively, we found element stresses in our heterogeneous samples of 0.8 ± 0.5 MPa in Sample 1, 2.50 ± 1.61 MPa in Sample 2, and 2.10 ± 1.56 MPa in Sample 3. In contrast, element stresses in the homogeneous case were 0.770 ± 0.062 MPa for Sample 1, 1.70 ± 0.15 MPa for Sample 2, and 1.680 ± 0.145 MPa in Sample 3. The bending stresses and free-edge displacements are summarized in **Table 1**. Note, under bending, errors in mean stress were as large as 32% when ignoring heterogeneity in tissue thickness.

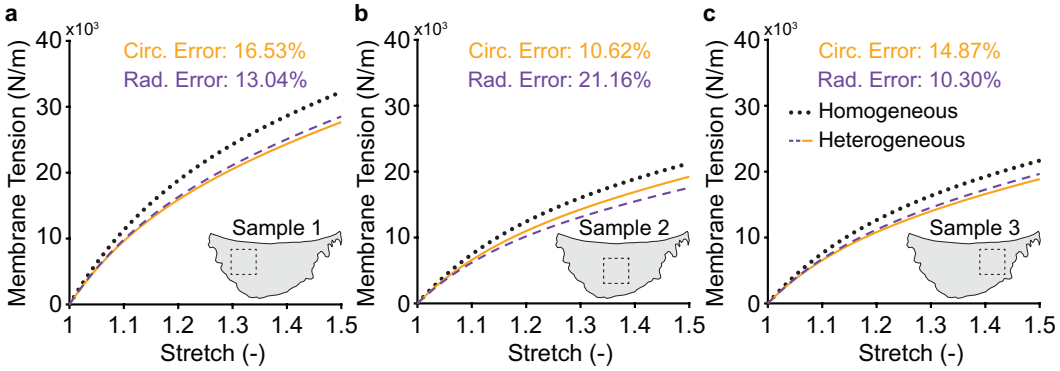

Fig. 5 Assuming homogeneity in tissue thickness leads to significant errors in the predicted constitutive response of anterior mitral valve leaflet tissue. a-c) Predicted biaxial response of three virtual tissue samples under the assumption of homogeneity in tissue thickness versus the predicted biaxial response of the same samples with the true, spatially-varying thickness distributions.

3.5 Assuming homogeneity also accrues significant errors in the buckling response of an anterior mitral valve leaflet

In a third test, we simulated the deformation of the anterior mitral valve leaflet in response to buckling using only one virtual sample. We repeated this simulation twice, assuming homogeneity or applying a true, spatially-varying thickness distribution. As expected at this point, we found that the response between the two simulations differed, see **Figure 6c**. Specifically, when looking qualitatively at the first three buckling modes, we found significant deviations in the size, shape, and location of displacements. Notably, the buckling deformations of the heterogeneous sample were localized in the sample's thinnest regions. Quantitatively, we saw a divergence in eigenvalues corresponding to each buckling mode between the two cases. Specifically, the homogeneous sample buckled in the first mode at a load factor – i.e. eigenvalue – of 10.081 as compared to an eigenvalue of 4.4375 in the heterogeneous case. Moreover, for the homogeneous case the second and third buckling modes were degenerate, they shared a common eigenvalue of 13.278, and were thus equally likely deformations. In contrast, the second and third buckling modes of the heterogeneous sample possessed distinct eigenvalues of 4.7615 and 4.9964, respectively. In other words, the second mode occurred before the third, see **Table 2**. Overall, ignoring heterogeneity in a buckling analysis lead to widely inaccurate results.

4 Discussion

Soft tissues are infamously heterogeneous. That is, their physical properties vary with location. Nonetheless, most biomechanical analyses of soft tissues ignore their heterogeneity; likely because of experimental hurdles. For example, measuring heterogeneous thicknesses of soft tissues is non-trivial. Therefore, our goal for this work was two-fold: First, our goal was to develop a technique to quickly capture non-destructive, continuous maps of soft tissue thickness under high-resolution. Our second goal was to apply this technique and to demonstrate the importance in considering thickness heterogeneity in biomechanical analysis of soft tissues.

We accomplished our first goal using a optical profilometry microscope. Specifically, we showed that soft tissues speckled with talcum powder provide enough contrast to optically create continuous, high-resolution thickness maps. Importantly, this imaging protocol is fast, taking only ten minutes for a $5\,\mathrm{cm}^2$ sample at $50\times$ magnification. We also demonstrated that this technique does not affect the mechanics of the tissue by repeated biaxial tests before applying our imaging protocol and after. Lastly, we successfully validated our findings against a mechanical thickness gauge. Together, our technique overcomes the short-comings of other, more traditional methods such as optical coherence tomography, histology, echocardiography, or thickness gauges.

We accomplished our second goal by using an example thickness map to conduct virtual mechanical tests. Specifically, we virtually excised three square samples from the high-resolution thickness map of an ovine anterior mitral valve leaflet. On these samples, we conducted planar biaxial tests, bending tests, and a buckling analyses. Please note that we chose these deformations as representative in-vivo loading modes of mitral valve tissue [29,27]. Importantly, for each analysis we compared the predictions when assuming a homogeneous thickness or using the true, spatially-varying thickness map. We found that assuming homogeneity can lead to widely inaccurate predictions under all three

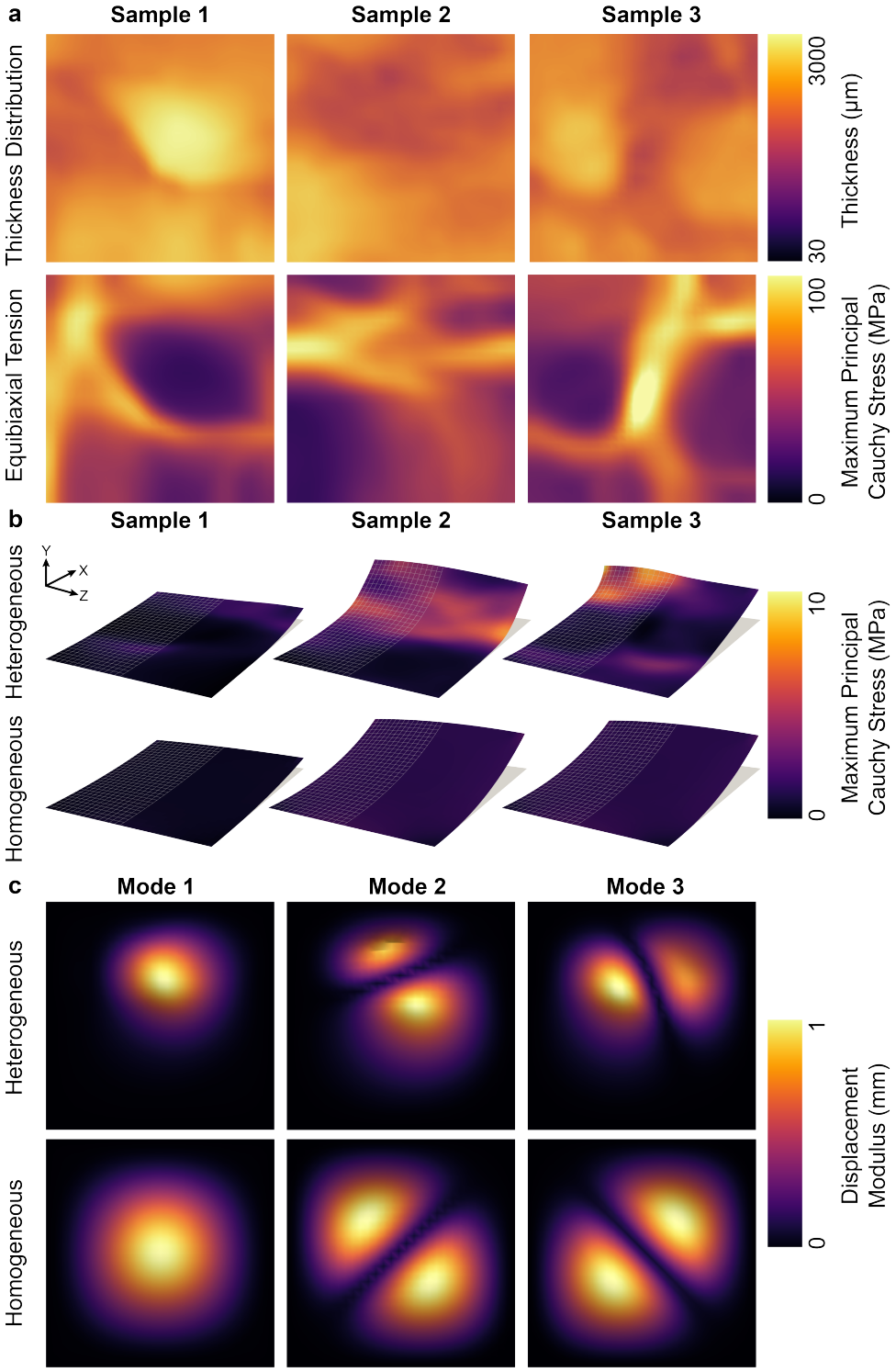

Fig. 6 Assuming homogeneity in thickness leads to significantly different material response in biaxial tension, bending, and buckling of anterior mitral valve leaflet tissue. a) Under biaxial tension, assuming homogeneous thickness leads to disparate results in stress fields. b) Under bending, assuming homogeneous thickness leads artificial stiffening and a smaller tip displacement as well as inaccurate stress fields. c) Under buckling, assuming homogeneous thickness leads to wrong predictions of the buckling modes. Please note, thickness data is mapped to a logarithmic scale.

Table 1 Assuming homogeneity in tissue thickness leads to significant errors in our tissue's bending response.

Sample	Thickness	Free-edge Displacement						Displacement Error		Maximum Principal			Stress
		X (mm)			Y (mm)			X (%)	Y (%)	Cauchy Stress (MPa)			Error (%)
Sample 1	Homogeneous	−0.0217	±	0.00174	0.472	±	0.0174	13.2	0.64	0.77	±	0.062	3.75
	Heterogeneous	−0.025	±	0.008	0.469	±	0.031	-	-	0.8	±	0.5	-
Sample 2	Homogeneous	−0.246	±	0.0171	1.57	±	0.051	60.32	19.49	1.7	±	0.15	32
	Heterogeneous	−0.62	±	0.07	1.95	±	0.17	-	-	2.5	±	1.61	-
Sample 3	Homogeneous	−0.221	±	0.0156	1.49	±	0.049	30.94	0.67	1.68	±	0.145	20
	Heterogeneous	−0.32	±	0.149	1.5	±	0.2	-	-	2.1	±	1.56	-

Table 2 Assuming homogeneity in tissue thickness leads to significant errors in our tissue's buckling response.

Mode	Thickness	Eigenvalue
Mode 1	Homogeneous	10.081
	Heterogeneous	4.4375
Mode 2	Homogeneous	13.278
	Heterogeneous	4.7615
Mode 3	Homogeneous	13.278
	Heterogeneous	4.9964

deformation modes. Most surprising to us was the magnitude of errors that could be accrued ranging from 21% under biaxial tension up to 60% under bending. Such errors likely exceed many other effects, including disease or treatment effects, and could thus mask important findings in biomechanical analyses.

Together, accomplishing our two goals represents an important contribution to the soft tissue biomechanics literature. That is, while most of us likely expected that we should include thickness heterogeneity in our analyses, the magnitude of errors we accrue by assuming homogeneity was surprising to us. Combined with our tangible and easy imaging protocol, we hope to not only inspire but also enable others to include thickness heterogeneity in their future biomechanical analyses. It should also be noted that our speckling protocol is not only useful when being used in combination with a Kayence scope, but can likely also be applied to other, laser-based thickness measurement techniques.

Of course, our work, like all others, is subject to limitations. Most importantly, we tested our protocols against only one type of soft tissue: ovine anterior mitral valve leaflet. Thus, others may repeat similar analyses as ours on their favorite soft tissue. However, we would like to highlight that our tissue of choice represents other tissues well in that it is highly hydrated, highly collageneous, semi-transparent, and, of course, soft [11]. In other words, we believe our tissue represents other tissues reasonably well. Also, please note that we demonstrated the importance of heterogeneous thickness maps using only virtual means. We did so because it allowed us to directly contrast the assumption of homogeneity with using true, spatially-varying thickness maps, which would not be possible experimentally. However, that also means that our findings are subject to the usual limitations of computational simulations. For example, we modeled our materials as hyperelastic and ignored time-dependent, viscoelastic effects etc. [12]. Finally, we only considered one type of heterogeneity in our current work: that of thickness. Of course, our tissue likely also demonstrates other forms of heterogeneity, for example in stiffness. We will explore the importance of heterogeneity in stiffness similarly to this current work in the future.

In conclusion, we introduced a non-destructive, fast method to obtain continuous, high-resolution thickness maps of soft tissues. We validated our technique against thickness gauge measurements and demonstrated this technique on an ovine anterior mitral valve leaflet. Importantly, we also showed that our imaging protocol does not affect the mechanics of soft tissues. Finally, we used our high resolution thickness map of an ovine anterior mitral valve leaflet to demonstrate the importance of including thickness heterogeneity in biomechanical analysis. Thereby, we showed that assuming homogeneity accrues significant errors under all three deformations modes. Thus, we recommend that biomechanicians consider thickness heterogeneity in their future analyses and hope they will use our technique to do so.

Acknowledgements

We acknowledge support by the American Heart Association through awards to Dr. Rausch (18CDA34120028) and a predoctoral fellowship to Mrudang Mathur (902502), as well as the National Institutes of Health through an award to Dr. Rausch (1R21HL161832). We would also like to thank Dr. Krishnaswamy Ravi-Chandar and Jinlong Guo for their assistance with the Keyence scope.

Author Contribution Statement

M.R., Mr.Ma., and C-Y.L. wrote the main manuscript. M.M. and C-Y.L. prepared all figures. Ma.Ma. and T.T. collected the animal tissue. All authors reviewed the manuscript.

Disclosures

Dr. Rausch has a speaking agreement with Edwards Lifesciences. None of the other authors have conflicts of interest to disclose.

References

1. Aumann, S., Donner, S., Fischer, J., Müller, F.: Optical Coherence Tomography (OCT): Principle and Technical Realization. In: J.F. Bille (ed.) High Resolution Imaging in Microscopy and Ophthalmology: New Frontiers in Biomedical Optics, pp. 59–85. Springer International Publishing, Cham (2019)
2. Bersi, M.R., Acosta Santamaría, V.A., Marback, K., Di Achille, P., Phillips, E.H., Goergen, C.J., Humphrey, J.D., Avril, S.: Multimodality imaging-based characterization of regional material properties in a murine model of aortic dissection. Scientific reports **10**(1), 1–23 (2020)
3. Bersi, M.R., Bellini, C., Humphrey, J.D., Avril, S.: Local variations in material and structural properties characterize murine thoracic aortic aneurysm mechanics. Biomechanics and modeling in mechanobiology **18**(1), 203–218 (2019)
4. Buerzle, W., Haller, C., Jabareen, M., Egger, J., Mallik, A., Ochsenbein-Koelble, N., Ehrbar, M., Mazza, E.: Multiaxial mechanical behavior of human fetal membranes and its relationship to microstructure. Biomechanics and modeling in mechanobiology **12**(4), 747–762 (2013)
5. Chen, S., Ní Annaidh, A., Roccabianca, S.: A microstructurally inspired constitutive model for skin mechanics. Biomechanics and modeling in mechanobiology **19**(1), 275–289 (2020)
6. Evkin, A.Y., Lykhachova, O.V.: Design buckling pressure for thin spherical shells: Development and validation. International Journal of Solids and Structures **156-157**, 61–72 (2019). DOI 10.1016/j.ijsolstr.2018.06.035
7. Farzaneh, S., Trabelsi, O., Avril, S.: Inverse identification of local stiffness across ascending thoracic aortic aneurysms. Biomechanics and Modeling in Mechanobiology **18**(1), 137–153 (2019)
8. Ferruzzi, J., Madziva, D., Caulk, A., Tellides, G., Humphrey, J.: Compromised mechanical homeostasis in arterial aging and associated cardiovascular consequences. Biomechanics and modeling in mechanobiology **17**(5), 1281–1295 (2018)
9. Fuentes, D., Thompson, E., Jacobsen, M., Crouch, A.C., Layman, R.R., Riviere, B., Cressman, E.: Imaging-based characterization of convective tissue properties. International Journal of Hyperthermia **37**(3), 155–163 (2020)
10. Ge, X.j., Zhang, L., Xiang, G., Hu, Y.c., Lun, D.x.: Cross-Sectional Area Measurement Techniques of Soft Tissue: A Literature Review. Orthopaedic Surgery **12**(6), 1547–1566 (2020)
11. Hasan, A., Ragaert, K., Swieszkowski, W., Selimovic, S., Paul, A., Camci-Unal, G., Mofrad, M.R.K., Khademhosseini, A.: Biomechanical properties of native and tissue engineered heart valve constructs. Journal of Biomechanics **47**(9), 1949–1963 (2014)
12. Holzapfel, G.A., et al.: Biomechanics of soft tissue. The handbook of materials behavior models **3**(1), 1049–1063 (2001)
13. Hughes, T.J., Liu, W.K.: Nonlinear finite element analysis of shells-part II. two-dimensional shells. Computer Methods in Applied Mechanics and Engineering **27**(2), 167–181 (1981). DOI 10.1016/0045-7825(81)90148-1
14. Jana, S., Lerman, A.: Behavior of valvular interstitial cells on trilayered nanofibrous substrate mimicking morphologies of heart valve leaflet. Acta Biomaterialia **85**, 142–156 (2019)
15. Jett, S., Laurence, D., Kunkel, R., Babu, A.R., Kramer, K., Baumwart, R., Towner, R., Wu, Y., Lee, C.H.: An investigation of the anisotropic mechanical properties and anatomical structure of porcine atrioventricular heart valves. Journal of the Mechanical Behavior of Biomedical Materials **87**, 155–171 (2018)
16. Joda, A., Jin, Z., Haverich, A., Summers, J., Korossis, S.: Multiphysics simulation of the effect of leaflet thickness inhomogeneity and material anisotropy on the stress-strain distribution on the aortic valve. Journal of Biomechanics **49**, 2502–2512 (2016)
17. Lee, C.H., Rabbah, J.P., Yoganathan, A.P., Gorman, R.C., Gorman, J.H., Sacks, M.S.: On the effects of leaflet microstructure and constitutive model on the closing behavior of the mitral valve. Biomechanics and Modeling in Mechanobiology **14**(6), 1281–1302 (2015)
18. Luetkemeyer, C.M., Rosario, R.A., Estrada, J.B., Arruda, E.M.: Fiber splay precludes the direct identification of ligament material properties: Implications for acl graft selection. Journal of Biomechanics **113**, 110104 (2020)
19. Luetkemeyer, C.M., Scheven, U., Estrada, J.B., Arruda, E.M.: Constitutive modeling of the anterior cruciate ligament bundles and patellar tendon with full-field methods. Journal of the Mechanics and Physics of Solids **156**, 104577 (2021)
20. Mathur, M., Meador, W.D., Malinowski, M., Jazwiec, T., Timek, T.A., Rausch, M.K.: Texas TriValve 1.0 : A reverse-engineered, open model of the human tricuspid valve. Engineering with Computers (2022)
21. Meador, W.D., Mathur, M., Sugerman, G.P., Jazwiec, T., Malinowski, M., Bersi, M.R., Timek, T.A., Rausch, M.K.: A detailed mechanical and microstructural analysis of ovine tricuspid valve leaflets. Acta biomaterialia **102**, 100–113 (2020)
22. Meador, W.D., Sugerman, G.P., Story, H.M., Seifert, A.W., Bersi, M.R., Tepole, A.B., Rausch, M.K.: The regional-dependent biaxial behavior of young and aged mouse skin: A detailed histomechanical characterization, residual strain analysis, and constitutive model. Acta biomaterialia **101**, 403–413 (2020)
23. Moran, C.M., Thomson, A.J.W.: Preclinical Ultrasound Imaging—A Review of Techniques and Imaging Applications. Frontiers in Physics **8** (2020)
24. O'Leary, S.A., Doyle, B.J., McGloughlin, T.M.: Comparison of methods used to measure the thickness of soft tissues and their influence on the evaluation of tensile stress. Journal of Biomechanics **46**, 1955–1960 (2013)
25. Pham, T., Sulejmani, F., Shin, E., Wang, D., Sun, W.: Quantification and comparison of the mechanical properties of four human cardiac valves. Acta Biomaterialia **54**, 345–355 (2017)

26. Pokutta-Paskaleva, A., Sulejmani, F., DelRocini, M., Sun, W.: Comparative mechanical, morphological, and microstructural characterization of porcine mitral and tricuspid leaflets and chordae tendineae. Acta Biomaterialia **85**, 241–252 (2019)
27. Rausch, M.K., Famaey, N., Shultz, T.O., Bothe, W., Miller, D.C., Kuhl, E.: Mechanics of the mitral valve: A critical review, an in vivo parameter identification, and the effect of prestrain. Biomechanics and Modeling in Mechanobiology **12**(5), 1053–1071 (2013)
28. Sachs, D., Wahlsten, A., Kozerke, S., Restivo, G., Mazza, E.: A biphasic multilayer computational model of human skin. Biomechanics and modeling in mechanobiology **20**(3), 969–982 (2021)
29. Sacks, M.S., Yoganathan, A.P.: Heart valve function: a biomechanical perspective. Philosophical Transactions of the Royal Society B: Biological Sciences **362**(1484), 1369–1391 (2007)
30. Smith, K., Mathur, M., Meador, W., Phillips-Garcia, B., Sugerman, G., Menta, A., Jazwiec, T., Malinowski, M., Timek, T., Rausch, M.: Tricuspid chordae tendineae mechanics: insertion site, leaflet, and size-specific analysis and constitutive modelling. Experimental Mechanics **61**(1), 19–29 (2021)
31. Sree, V.D., Rausch, M.K., Tepole, A.B.: Linking microvascular collapse to tissue hypoxia in a multiscale model of pressure ulcer initiation. Biomechanics and modeling in mechanobiology **18**(6), 1947–1964 (2019)
32. Ud-Din, S., Foden, P., Stocking, K., Mazhari, M., Al-Habba, S., Baguneid, M., McGeorge, D., Bayat, A.: Objective assessment of dermal fibrosis in cutaneous scarring, using optical coherence tomography, high-frequency ultrasound and immunohistomorphometry of human skin. British Journal of Dermatology **181**(4), 722–732 (2019)
33. Witzenburg, C.M., Barocas, V.H.: A nonlinear anisotropic inverse method for computational dissection of inhomogeneous planar tissues. Computer methods in biomechanics and biomedical engineering **19**(15), 1630–1646 (2016)
34. Witzenburg, C.M., Holmes, J.W.: Predicting the time course of ventricular dilation and thickening using a rapid compartmental model. Journal of cardiovascular translational research **11**(2), 109–122 (2018)